

## Advantages of Electro-deposited Gold on Carbon Electrodes for NT-proBNP Immunosensor for Development of Heart Failure Test Kit

Pongsakorn Aiemderm, Kanchana Monkhang, Sureeporn Wongiard, Kiattawee Choowongkomon and Napachanok Mongkoldhumrongkul Swainson\*  
Department of Biochemistry, Faculty of Science, Kasetsart University, Bangkok, Thailand

Chaiya Prasittichai  
Department of Chemistry, Faculty of Science, Kasetsart University, Bangkok, Thailand  
Center of Excellence for Innovation in Chemistry, Faculty of Science, Kasetsart University, Bangkok, Thailand

Charoenkwan Kraiya  
Electrochemistry and Optical Spectroscopy Center of Excellence, Department of Chemistry, Faculty of Science, Chulalongkorn University, Pathumwan, Bangkok, Thailand

\* Corresponding author. E-mail: napachanok.m@ku.ac.th DOI: 10.14416/j.asep.2023.10.004  
Received: 8 June 2023; Revised: 6 July 2023; Accepted: 20 July 2023; Published online: 5 October 2023  
© 2023 King Mongkut's University of Technology North Bangkok. All Rights Reserved.

### Abstract

Accurate measurement of the N-terminal pro B-type natriuretic peptide (NT-proBNP) in serum is important for the diagnosis of heart failure (HF). Carbon screen-printed electrodes (SPCEs) modified with graphene oxide (GO) or gold (Au) were compared for the construction of NT-proBNP immunosensors. NT-proBNP and its recognition unit, a single-chain variable fragment fused with alkaline phosphatase (scFv-AP), were expressed and purified. The currents of the electrodes immobilized with scFv-AP were measured after adding an ethanolamine (ETA), blank and NT-proBNP in either phosphate buffer saline (PBS) or human serum. SPCE/Au had lower mean baseline slopes than for SPCE/GO for all measurements, in both PBS and serum, indicating greater accuracy for SPCE/Au. None of the measurements in PBS had statistically different peak currents between SPCE/GO and SPCE/Au; however, there was a significant difference with the serum. The significant reduction of SPCE/GO peak currents after applying serum blank implied non-specific absorption on the surface. The peak current of 300 pg/mL of NT-proBNP in the serum measured on SPCE/Au was significantly higher (by a factor of three) than on SPCE/GO, suggesting the possibility of using SPCE/Au to detect NT-proBNP at higher concentrations. The binding efficiency of scFv-AP to NT-proBNP did not depend on the electrodes, as shown by the similar delta peak-currents (Blank-Target). Thus, immobilized scFv-AP on SPCE/Au electrodes had good potential to accurately detect NT-proBNP in serum, for use in the fabrication of an HF test kit.

**Keywords:** NT-proBNP, Heart failure, Graphene oxide, Gold nanoparticles, Biosensor, scFv

### 1 Introduction

Heart failure (HF) is an abnormality of cardiac function leading to inefficiency in contract-relax activity and pumping the blood to various organs. Thus rapid diagnosis of HF is important before it becomes fatal. Not only that such diagnosis increase the patient

survival rate, it will also save on the time and cost of treating patients [1].

Brain or B-type natriuretic peptide (BNP) is a hormone released from the ventricles of the heart into the bloodstream when wall stress occurs. It is produced in the form of pro-hormone or proBNP before being cut into an N-terminal part (NT-proBNP) and

BNP [2]. Commonly, NT-proBNP is used in clinical measurement to reference HF because of its longer half-life [3], compared to BNP. The cutoff amount of NT-proBNP to diagnose chronic HF is above 300 pg/mL [1].

A single-chain variable fragment (scFv) is an engineered immunoglobulin (generated by the fusion of heavy ( $V_H$ ) and light chain ( $V_L$ ) domains) that has antigen binding activities. An scFv specific to any particular antigen can be selected and generated using a phage display technique [4]. Our laboratory produced an scFv specifically to bind to the C-terminal part of NT-proBNP that showed potential for use as a recognition unit on an immunosensor [5].

Electrochemical biosensors have been used for point-of-care testing (POCT), for example, blood glucose tests, because they have high sensitivity and low detection limits. Combined with a recognition unit, such as DNA aptamers [6], antibodies, and scFvs, the technique acquires specificity and accuracy [7]. Basically, this method measures the current or peak current changes in an electrolyte solution after the binding of the target to a recognition element deposited on the working electrode (WE) surface of the sensors [8]. Measurement is usually performed using electrochemical techniques, such as amperometry, potentiometry, and voltammetry, for example, cyclic voltammetry (CV), linear sweep voltammetry, and square wave voltammetry (SWV).

Screen printed electrodes (SPEs) are used in many electrochemical biosensors because of their many applications in printing electronic devices directly on plastic materials. SPEs consist of three electrodes: a pseudo reference electrode (RE), a counter electrode (CE) and a WE. Often, the modification of the WE involves three procedures: mixing the ink with the modifier agent, electrochemical depositing a metal, and drop casting nanomaterials [9]. The drop-casting methods allow various types of materials to be applied to the WE.

Graphene is a carbon allotrope composed of a single layer of carbon with partially filled  $sp^2$  orbitals above and below the plane of the sheet [10], while graphene oxide (GO) is a two-dimensional, oxygenated, carbon nanosheet. GO can be reduced using either chemical reactions with different reagents or using an electrochemical method by applying a negative potential to reduce the oxygen functional group present

on the surface of the GO [11]. An advantage of GO as an electrochemical sensor is that it can be modified subsequently by N-hydroxysuccinimide ester (NHS) to immobilize antibodies [12].

The use of gold nanoparticles (AuNPs) in electrochemical biosensors has gained interest because of their high stability, high surface-to-volume ratio, excellent electroconductivity, and stable immobilization of biomolecules [13]. AuNPs bind to biomolecules on the electrode surface through the thiol functional group [14]. Thus, cysteamine is used as a linking agent that is spontaneously chemi-absorbed on the metallic surface. It exposes amine ( $-NH_2$ ) moieties on the other side of the molecule for further immobilization using 1-ethyl-3-(3-dimethylaminopropyl)-carbodiimide (EDC)/NHS [15].

Another study compared absorbing DNA aptamer probes on a screen print carbon electrode (SPCE) that were deposited with either GO (SPCE/GO) or AuNPs (SPCE/Au). The results showed the advantage of using SPCE/GO to immobilize the DNA aptamer but it had higher non-specificity than SPCE/Au [16]. However, to date, there has been no evaluation of the types of SPCE modification to immobilize protein on the surface.

Consequently, the present work compared SPCE/GO and SPCE/Au immobilized with scFv protein. The target, NT-proBNP, and the scFv-AP were produced. Then, scFvs were immobilized on the WE to measure the amount of NT-proBNP in the phosphate buffer saline (PBS) and serum. The currents at the electrodes were measured for a blank and for 300 pg/mL of NT-proBNP. The baselines of the current and peak currents were analyzed to evaluate which types of electrodes should be used for the development of an electrochemical immunosensor for HF detection.

## 2 Materials and Methods

### 2.1 Reagents and chemicals

1-Ethyl-3-(3-dimethylaminopropyl) carbodiimide (EDC) and N-hydroxysuccinimide (NHS) were purchased from Thermo Scientific. Graphene oxide nanocolloids (GO), potassium ferricyanide ( $K_3[Fe(CN)_6]$ ), potassium ferrocyanide ( $K_4[Fe(CN)_6]$ ), potassium chloride (KCl), gold (III) chloride ( $HAuCl_4$ ), cysteamine, and ethanolamine (ETA) were purchased from Sigma-Aldrich. Phosphate-buffered saline (PBS) was

purchased from Apsalagen. All solutions were prepared in ultrapure water (Sartorius).

## 2.2 Instrumentation

A PalmSens4 potentiostat was used for all electrochemical analysis and electrode preparation. This instrument was controlled using the PSTrace 5.9 software. The SPCE (Quasense) was composed of a carbon working electrode (3 mm), a carbon counter electrode, and a silver/silver chloride reference electrode.

## 2.3 NT-proBNP expression and purification

The recombinant pET32a (+) NT-proBNP (Genorise<sup>®</sup>) was transformed into *E. coli* BL21 (DE3) based on heat shock; then, a single colony from the selection plate was inoculated into 3 mL Luria-Bertani (LB) medium containing 50 µg/mL ampicillin and shaken overnight at 30 °C. The starter at 1% was then transferred to a larger-scale LB medium (250 mL LB broth containing 50 µg/mL ampicillin) and incubated at 37 °C for around 4 h until reaching OD<sub>600</sub> = 0.5–0.7. Next, isopropyl β-D-thiogalactopyranoside (IPTG) was added to a final concentration of 1 mM and incubated overnight at 30 °C. Later, the cells were collected using centrifugation at 4 °C, 10,000×g for 5 min. Cell pellets were resuspended in 100 µL PBS and stored at –20 °C until used. S-protein tagged NT-proBNP expressing cells were lysed by resuspending in lysis buffer (50 mM NaH<sub>2</sub>PO<sub>4</sub>, 300 mM NaCl, 10 mM imidazole, pH 8.0) containing 0.1 mg/mL lysozyme, incubated on ice for 30 min, and sonicated on ice (10 s bursts per 10 s cooling at 200–300 W, 6×). Then, the reaction was centrifuged at 4 °C, 10,000×g for 30 min. Soluble proteins in the supernatant were collected and loaded onto a HisPur Ni-NTA Superflow Agarose column (Thermo Scientific). The retained proteins of interest were eluted with elution buffer (50 mM NaH<sub>2</sub>PO<sub>4</sub>, 300 mM NaCl, 250 mM imidazole, pH 8.0) and the eluate was collected. Then, the S-protein tagged NT-proBNP was concentrated by spinning in a 3 kDa molecular weight cut-off column. Next, the 30 kDa proteins were incubated with S-protein agarose and specifically cleaved using enterokinase, resulting in 8.5 kDa NT-proBNP. Then, the S-protein tags and NT-proBNP were separated using centrifugation at

11,000×g for 10 mins at 4 °C. The NT-proBNP was collected from the supernatant and investigated based on Western blot analysis using HisProbe<sup>™</sup>-HRP (Thermo Scientific) as the recognition unit. NT-proBNP in a solution was exchanged with PBS buffer in a 3 kDa molecular weight cut-off column. The protein concentration was determined using the BCA protein assay kit (Thermo Scientific) and analyzed based on Sodium Dodecyl Sulphate-Polyacrylamide Gel Electrophoresis (SDS-PAGE). Finally, the NT-proBNP was dissolved in PBS or NT-proBNP free human serum (HyTest) at 300 pg/mL for analysis.

## 2.4 NT-proBNP specific scFv-AP expression and purification

The recombinant pSANG14-3F (Addgene 39265) containing NT-proBNP binding scFv that was fused with alkaline phosphatase (scFv-AP) was produced in the laboratory following the previous protocol in the laboratory [5]. Briefly, scFv-AP was transformed into *E. coli* BL21 (DE3) using a heat shock method and cultured in LB (starter) medium containing 50 µg/mL kanamycin. Induction of protein expression was started by adding IPTG to a final concentration of 0.2 mM and incubating overnight at 16 °C. Then, the cells were collected using centrifugation at 7,600×g and 4 °C for 30 min, after which, the cell pellet was weighed. Expressed proteins in periplasm were collected by resuspending the cell pellet in hypertonic solution (30 mM Tris-HCl, 20% sucrose, and 1 mM EDTA, pH 8) and incubating on ice for 30 min. After centrifugation at 7,600×g and 4 °C for 30 min and collecting the supernatant, the remaining pellets were resuspended in hypotonic solution (5 mM MgSO<sub>4</sub>) and incubated on ice for 30 min. After centrifugation at 7,600×g and 4 °C for 30 min, the supernatant of the hypotonic solution was collected and pooled with the previous supernatant of the hypertonic solution. Then, the collected supernatant was centrifuged at 7,600×g and 4 °C for 30 min to remove any debris, after which, the supernatant was passed through a 0.45 µm filter and dialyzed using 3.5 K MWCO dialysis tubing (Thermo Scientific) with buffer A (20 mM Tris-HCl, 300 mM NaCl, 10 mM imidazole, and 0.1 mM PMSF, pH 8). The protein mixture in buffer A was purified using a HisPur Ni-NTA Superflow Agarose column. The retained protein of interest was eluted with elution

buffer (20 mM Tris-HCl, 300 mM NaCl, 100 mM imidazole, pH 8.0) and the eluate was collected. Purified proteins were concentrated and the buffer was exchanged with PBS using a 3 kDa molecular weight cut-off column. The protein concentration was determined using a BCA protein assay kit and analyzed based on SDS-PAGE and Western blot.

## 2.5 Preparation of SPCE/GO

To prepare a homogeneous suspension, the aqueous solution of 0.5 mg/mL GO was prepared in PBS and sonicated for 1 h. The prepared solution was carefully deposited onto the surface of an SPCE (Quasense) and dried for 30 min at 50 °C. Next, the GO layer was electrochemically reduced in PBS using 5 CV cycles. The potential was used in the range  $-1.5$  to  $0$  V and a scan rate of 100 mV/s was applied. After that, the SPCE/GO was washed once with ultrapure water. Next, the working electrode (WE) of an SPCE/GO was incubated in 100 mM NHS in PBS for 30 min at 37 °C. Subsequently, the electrodes were washed once with PBS. The WE of the SPCE/GO was incubated for 30 min in 22.5 ng/mL of scFv-AP at room temperature. After that, the electrodes were washed once with PBS to remove any unbound scFv-AP. Following this, the surface was blocked with 1 M ethanolamine (ETA) for 10 minutes at room temperature and washed once with PBS before proceeding to the electrochemical measurement step.

## 2.6 Preparation of SPCE/Au

All SPCEs were activated using CV for 40 cycles at a scanning potential of  $-0.6$  to  $1.6$  V and a scan rate of 100 mV/s in PBS. The SPCEs were then washed once with ultrapure water. The electrode was cleaned by drop-casting with 500 mM  $H_2SO_4$  and CV scanning for 5 cycles at a scan rate of 100 mV/s, with a potential in the range  $-0.1$  to  $1.3$  V. Subsequently, an electrochemical deposition of AuNPs on the SPCE was performed using chronoamperometry at an applied potential of  $-0.4$  V for 180 s in a solution containing 0.5 mM  $H AuCl_4$  and 500 mM  $H_2SO_4$ . After the deposition, the electrodes were washed once with ultrapure water. Next, the SPCE/Au was incubated overnight in 2.5 mM cysteamine in PBS at room temperature in darkness. The electrode was washed

once with PBS. Later, 100 mM EDC, 25 mM NHS, and 22.5 ng/mL scFv-AP (volume ratio: 0.5:0.5:1) composite was drop-cast onto the WE of the Au-SPCE for 30 min at room temperature. The electrodes were then washed once with PBS to remove any unbound EDC/NHS and scFv-AP. To block non-specific binding on the surface, 1 M ETA was applied for 10 min at room temperature and washed once with PBS before continuing the next step.

## 2.7 Electrochemical measurements

All measurements were carried out in an electrolyte solution containing 5 mM potassium ferro/ferricyanide solution with 100 mM KCl as the supporting electrolyte. PBS or NT-proBNP-free human serum was used as a blank control. SWV was measured from  $-0.2$  to  $0.6$  V with a step potential of 0.003 V and an applied amplitude of 0.08 V at a frequency of 8 Hz. The currents and peak currents were analyzed using the PStTrace software.

## 2.8 Statistical analyses

A two-tailed nonparametric Mann-Whitney test was used to compare the peak currents and the baseline slopes between SPCE/GO and SPCE/Au.

## 3 Results and Discussion

### 3.1 Production of NT-proBNP

After IPTG induction at 30 °C and purification using an affinity Ni column, each fraction was visualized based on 12% SDS-PAGE [Figure 1(a)]. The results showed a high purity fraction (with a band of approximately 30 kDa) was eluted after 4 times. Fractions of S-protein tagged NT-proBNP were concentrated and cleaved at specific sites using enterokinase while bound on S-protein agarose. These results showed the two expected cleaved products (at  $\sim 17$  kDa and  $\sim 11$  kDa). The released NT-proBNP at approximately 11 kDa was separated from the S-agarose using centrifugation and detected by Western blot analysis [Figure 1(b)]. The yield of NT-proBNP production was 0.1 mg/L of cell culture. Although the produced NT-proBNP did not contain glycosylation because it was produced in bacteria, the target site of scFv-AP binding was in

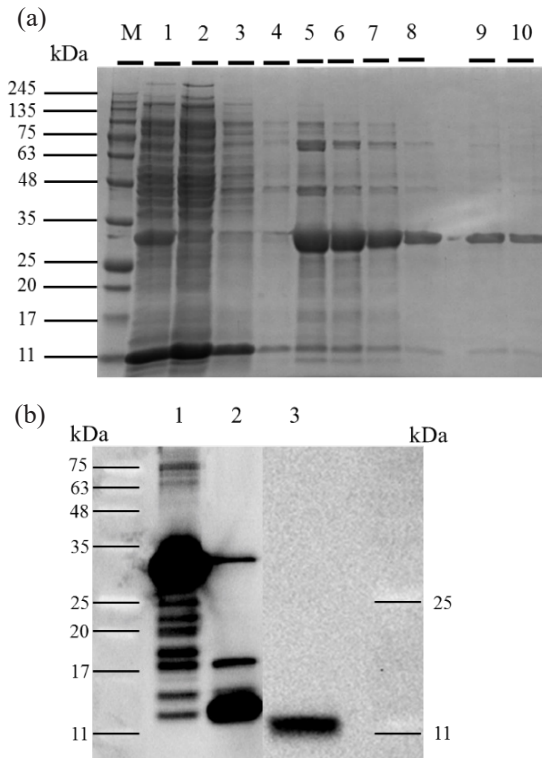


**Figure 1:** NT-proBNP production (a) SDS-PAGE analysis of purified S-protein tagged NT-proBNP using affinity Ni column (M: protein marker, 1: Clear lysate, 2: Flow through, 3–4: Washes 1 and 2, respectively, 5–10: NT-proBNP fraction eluted using imidazole with concentration 250 mM. (b) Western blot analysis of NT-proBNP specifically cleaved using enterokinase (1: NT-proBNP eluted fraction, 2: Enterokinase cleavage product, 3: ~11 kDa NT-proBNP after centrifugation separation).

the region of 51–76 amino acids, which were non-glycosylation sites in unique regions to differentiate proBNP from NT-proBNP in the plasma [17].

### 3.2 Production of NT-proBNP specific scFv-AP

The expressed scFv-AP at 16 °C was purified using an affinity Ni column. Every fraction was visualized based on 12% SDS-PAGE [Figure 2(a)]. The scFv with alkaline phosphatase fusion had a size of approximately 70 kDa. Figure 2(b) shows that there were 2 sizes of detected proteins. The additional size could have been the size of pelB (2.23 kDa) which was at the N-terminal

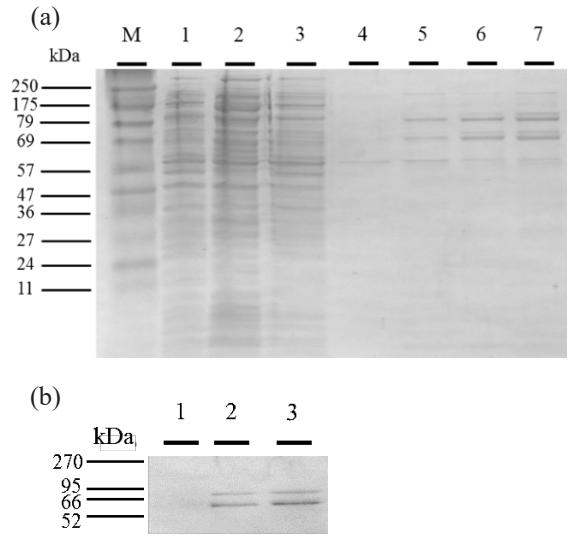


**Figure 2:** Production of NT-proBNP-specific scFv-AP (a) SDS-PAGE analysis of purified NT-proBNP-specific scFv-AP (M: protein marker, 1: Before dialysis, 2: Pellet, 3: Flow through, 4: Wash, 5–7: scFv-AP fraction eluted using imidazole with concentrations of 5%, 10%, and 20% of 100 mM imidazole in buffer A. (b) Western blot analysis of ~70 kDa NT-proBNP-specific scFv-AP expressed product (1–3: scFv-AP fraction eluted using imidazole with concentrations of 5%, 10%, and 20% of elution buffer in buffer A).

of the expressed proteins and could be cleaved at periplasm [18]. NT-proBNP-specific scFv-AP production was 0.5 mg/L of cell culture.

### 3.3 Modification of SPCE

The SPCE was modified using GO and AuNPs due to their ability to immobilize a recognition-unit protein on the surface. First, the SPCE was modified using drop-casting and electrochemically reduced GO and then the scFv-AP protein was immobilized on the surface, similar to Sethi and colleagues [12]. The immobilized H31L21 antibody SPCE/GO had detected the A $\beta$ 1-42 biomarker in the plasma with the limit of detection (LOD) at 2.40 pM. Second, the SPCE was electrochemically deposited with AuNPs and the scFv-AP was immobilized on the surface, similar to Amor-Gutierrez and colleagues [19]. The PAb240 antibody was immobilized using chemisorption on the surface to competitively detect p53 in the serum



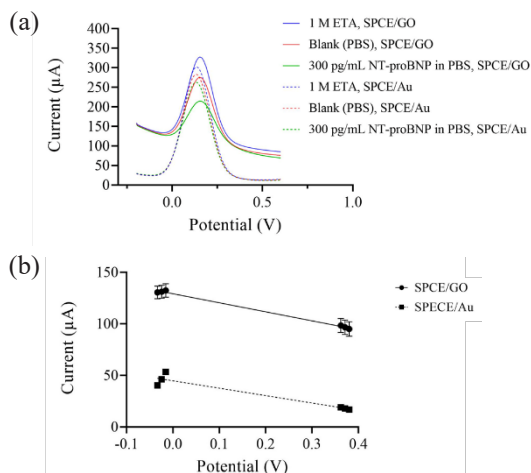


**Figure 3:** Electrochemical analysis in PBS (a) Square wave voltammogram of SPCE/GO (solid lines) and SPCE/Au (dash lines) (b) Slopes of baselines of SPCE/GO and SPCE/Au. The experiments were carried out using 3 electrodes for every measurement. Mann-Whitney test showed a significant difference in slope values at  $p < 0.0001$ .

at an LOD value of 0.05 nM. In the current study, scFv-AP was successfully immobilized on the surface of SPCE/GO and SPCE/Au, followed by being blocked using ETA.

The electrochemical responses of the electrodes were observed after adding ETA, PBS or serum blank, and NT-proBNP in the PBS or serum. A reduction in the current was expected because the resistance was increased by the presence of the analysts on the surface of the electrodes. The baseline current of the voltammograms is important for accurate measurement of the true peak currents. When the baseline has a steep slope and non-linear character, the calculated peak magnitude is likely to be inaccurate, especially with low analytical signals [20].

### 3.4 Electrochemical sensing of NT-proBNP in PBS

The voltammograms of SPCE/GO and SPCE/Au ( $n = 3$ ) after adding ETA, PBS blank, and NT-proBNP in PBS are shown in Figure 3(a). Reductions in the peak currents after each step were observed in both SPCE/GO and SPCE/Au. In addition, the average current of measurements ( $n = 9$ ) was calculated at potentials of  $-0.0334$ ,  $-0.0244$ ,  $-0.01551$ ,  $0.362384$ ,  $0.37129$ , and

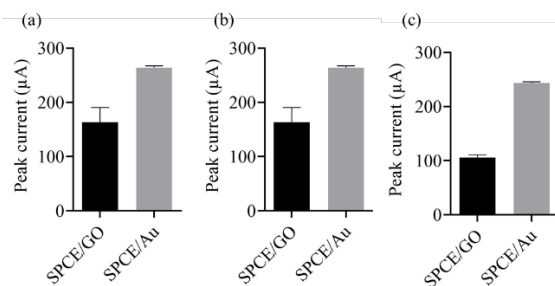


**Figure 4:** Comparative analysis of peak current of (a) ETA, (b) PBS blank, and (c) 300 pg/mL of NT-proBNP in PBS. Bars represent mean  $\pm$  SD. Data was analyzed using the Mann-Whitney test.

$0.380197$  V to construct the average baselines and calculate their slopes [Figure 3(b)]. The linear equation of the baselines of SPCE/GO was  $y = -87.635x + 129.25$  ( $R^2 = 0.9959$ ) and for SPCE/Au was  $y = -71.87x + 44.776$  ( $R^2 = 0.9207$ ). Statistical analysis revealed that SPCE/Au had a highly significantly ( $p < 0.0001$ ) lower slope than SPCE/GO.

### 3.5 Comparative analysis of peak current of NT-proBNP in PBS

The peak currents of measurements were compared between SPCE/GO and SPCE/Au (Figure 4). While there were no significant differences among them, there was a trend for a higher peak current of 300 pg/mL NT-proBNP detected on SPCE/Au. The differences in the peak currents of PBS blank and NT-proBNP were  $57.62 \pm 31.41$  and  $20.60 \pm 0.99$   $\mu\text{A}$  for SPCE/GO and SPCE/Au, respectively, with a notably high standard deviation value when SPCE/GO was used.

### 3.6 Electrochemical sensing of NT-proBNP in serum

Voltammograms of SPCE/GO and SPCE/Au ( $n = 5$ ) after adding ETA, serum blank, and NT-proBNP in serum are shown in Figure 5(a). A reduction in the peak currents after each step remained in both SPCE/GO and SPCE/Au. Furthermore, the average currents of measurements ( $n = 15$ ) were calculated at the same potential as analyzed for PBS ( $-0.0334$ ,  $-0.0244$ ,  $-0.01551$ ,  $0.362384$ ,  $0.37129$ , and  $0.380197$  V). The average baselines were constructed and linear equations were calculated to determine their slopes [Figure 3(b)]. The linear equation of the baselines of

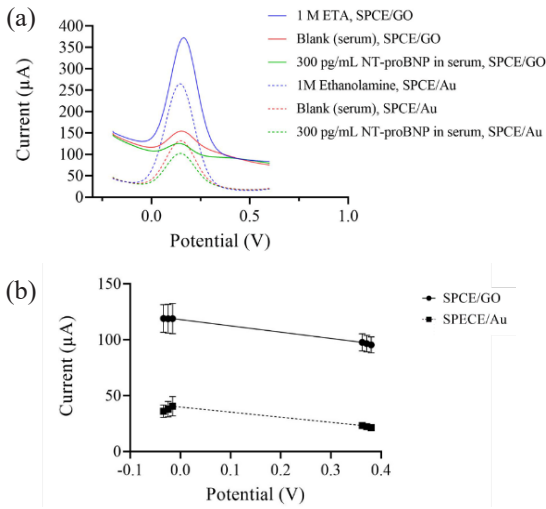


**Figure 5:** Electrochemical analysis in human serum (a) Square wave voltammogram of SPCE/GO (solid lines) and SPCE/Au (dash lines) (b) Slopes of baselines of SPCE/GO and SPCE/Au. The experiments were carried out using 5 electrodes for every measurement. Mann-Whitney test showed a significant difference in slope values at  $p = 0.0145$ .

SPCE/GO was  $y = -56.43x + 117.53$  ( $R^2 = 0.9985$ ) and of SPCE/Au was  $y = -39.86x + 37.19$  ( $R^2 = 0.9625$ ).

The comparative analysis of baseline slopes indicated SPCE/Au had a significantly lower slope and greater linearity compared to SPCE/GO for the analysis in serum ( $p = 0.0145$ ), similar to the abovementioned analysis in PBS. Thus, it could be concluded that SPCE/Au produced a more accurate estimate of the true peak current [20].

### 3.7 Comparative analysis of peak current of NT-proBNP in serum

For the analysis in human serum, the peak currents of every measurement were compared between SPCE/GO and SPCE/Au (Figure 6). The results indicated there were no significant differences only after ETA was applied. However, when serum blank was added, there was a substantial reduction in the peak current on SPCE/GO that was significantly different from the peak current of SPCE/Au ( $p = 0.0079$ ,  $n = 5$ ). The peak currents of SPCE/GO and SPCE/Au were  $47 \pm 4.3$  and  $106 \pm 9.9 \mu\text{A}$ , respectively. The experimental results were consistent with those reported by Zhang

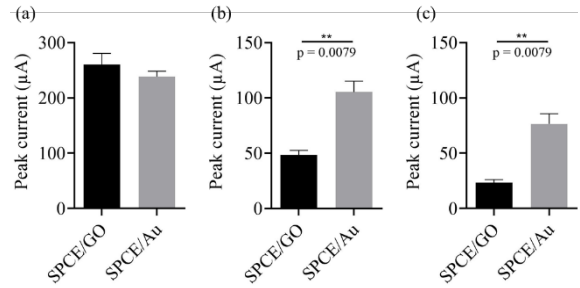


**Figure 6:** Comparative analysis of peak current of (a) ETA, (b) serum blank, and (c) NT-proBNP in serum. Bars represent mean  $\pm$  SD. Data was analyzed using the Mann-Whitney test.

and colleagues [16] that implied SPCE/GO had higher non-specific absorption by protein than SPCE/Au.

Further reductions in the peak currents were observed after 300 pg/mL of NT-proBNP in serum for both SPCE/GO and SPCE/Au. The peak currents after adding the target in the serum of SPCE/GO were significantly lower than those of SPCE/Au at  $23.87 \pm 3.15$  and  $76.51 \pm 9.15 \mu\text{A}$ , respectively ( $p = 0.0079$ ,  $n = 5$ ). The higher peak currents for SPCE/Au suggested the possibility of being able to distinguish any further current reduction if a higher concentration of NT-proBNP than 300 pg/mL was measured.

The differences in the peak currents of the serum blank and NT-proBNP in serum were  $24.73 \pm 2.74$  and  $28.82 \pm 2.93 \mu\text{A}$  for SPCE/GO and SPCE/Au, respectively. This revealed the affinity of the scFv-AP to NT-proBNP in serum, independent of the modification on the electrodes.

The current change of NT-proBNP at 300 pg/mL was investigated because it is the cutoff value for chronic HF at all ages [1]. For acute HF, the diagnosis values are categorized by age, with those for patients younger than 50 years, aged between 50 and 75, and those aged above 75 years being higher than 450, 900, and 1,800 pg/mL, respectively [21]. Thus, SPCE/Au using scFv-AP to recognize NT-proBNP has potential in the development of an HF test kit to evaluate chronic and acute HF.

## 4 Conclusions

NT-proBNP and NT-proBNP-specific scFv-AP were successfully produced in the current work. The average baseline slopes of SPCE/Au had lower values than for

SPCE/GO with measurements in both PBS and serum, indicating that SPCE/Au could produce a greater level of accuracy than SPCE/GO. Comparative analyses of the peak currents in PBS showed no significant differences between SPCE/GO and SPCE/Au. On the other hand, the experiments in serum blank resulted in significant differences due to the non-specific adsorption of proteins on the surface of SPCE/GO. Furthermore, there was a significantly higher peak current in SPCE/Au when measuring 300 pg/mL of NT-proBNP in serum. This indicated the possibility of developing a test kit to measure NT-proBNP at higher concentrations and its use for the diagnosis of acute HF in patients younger than 50 years. Thus, SPCE/Au was a more suitable biosensor that could immobilize the protein recognition unit of the WE and measure NT-proBNP in serum.

### Acknowledgments

This research project was financially supported by the National Research Council of Thailand (NRCT, grant number N34A650492) and Kasetsart University through the Graduate School Fellowship Program.

### Author Contributions

P.A.: investigation, methodology, data analysis, writing an original draft; K.M. and S.W.: investigation and methodology; C.P. and K.C.: conceptualization, reviewing and editing; C.K.: research design, conceptualization, reviewing and editing; N.M.S.: conceptualization, data curation, writing—reviewing and editing, funding acquisition, project administration. All authors have read and agreed to the published version of the manuscript.

### Conflicts of Interest

The authors declare no conflicts of interest.

### References

- [1] C. Mueller, K. McDonald, R. A. de Boer, A. Maisel, J. G. F. Cleland, N. Kozhuharov, A. J. S. Coats, M. Metra, A. Mebazaa, F. Ruschitzka, M. Lainscak, G. Filippatos, P. M. Seferovic, W. C. Meijers, A. Bayes-Genis, T. Mueller, M. Richards, and J. L. Januzzi Jr, “Heart Failure Association of the European Society of Cardiology practical guidance on the use of natriuretic peptide concentrations,” *European Journal of Heart Failure*, vol. 21, no. 6, pp. 715–731, 2019.
- [2] Y. Su Kim, N. Karisa, W. Y. Jeon, H. Lee, Y.-C. Kim, and J. Ahn, “High-level production of N-terminal pro-brain natriuretic peptide, as a calibrant of heart failure diagnosis, in *Escherichia coli*,” *Applied Microbiology and Biotechnology*, vol. 103, no. 12, pp. 4779–4788, 2019.
- [3] M. Weber, V. Mitrovic, and C. Hamm, “B-type natriuretic peptide and N-terminal pro-B-type natriuretic peptide - Diagnostic role in stable coronary artery disease,” *Experimental & Clinical Cardiology*, vol. 11, no. 2, pp. 99–101, 2006.
- [4] S. H. Wang, J. B. Zhang, Z. P. Zhang, Y. F. Zhou, R. F. Yang, J. Chen, Y. C. Guo, F. You, and X. E. Zhang, “Construction of Single Chain Variable Fragment (ScFv) and BiscFv-Alkaline phosphatase fusion protein for detection of *bacillus anthracis*,” *Analytical Chemistry*, vol. 78, no. 4, pp. 997–1004, 2006.
- [5] S. Wongjard, P. Aiemderm, K. Monkhang, K. Jaengwang, L. Tabtimmai, C. Kraiyya, K. Choowongkomon, and N. M. Swainson, “Selection, alkaline phosphatase fusion, and application of single-chain variable fragment (scFv) specific to NT-proBNP as electrochemical immunosensor for heart failure,” *Heliyon*, vol. 9, 2023, Art. no. e19710, doi: 10.1016/j.heliyon.2023.e19710.
- [6] N. M. Swainson, P. Aiemderm, C. Saikaew, K. Theeraraksakul, P. Rimdusit, C. Kraiyya, S. Unajak, and K. Choowongkomon, “Biosensors for the detection of organophosphate exposure by a new diethyl thiophosphate-specific aptamer,” *Biotechnology Letters*, vol. 43, no. 9, pp. 1869–1881, 2021.
- [7] Y. Liu and G. Dykstra, “Recent progress on electrochemical (bio)sensors based on aptamer-molecularly imprinted polymer dual recognition,” *Sensors and Actuators Reports*, vol. 4, 2022, Art. no. 100112.
- [8] S. Campuzano, M. Pedrero, P. Yáñez-Sedeño, and J. M. Pingarrón, “New challenges in point of care electrochemical detection of clinical biomarkers,”



- Sensors and Actuators B: Chemical*, vol. 345, 2021, Art. no. 130349.
- [9] G. Paimard, E. Ghasali, and M. Baeza, "Screen-printed electrodes: Fabrication, modification, and biosensing applications," *Chemosensors*, vol. 11, no. 2, 2023, Art. no. 113.
- [10] A. G. Crevillen, A. Escarpa, and C. D. García, "Carbon-based nanomaterials in analytical chemistry," in *Handbook of Smart Materials in Analytical Chemistry*. New Jersey: Wiley, pp. 345–374, 2019.
- [11] M. Zidan, R. M. Zawawi, M. Erhayem, and A. Salhin, "Electrochemical detection of paracetamol using graphene oxide -modified glassy carbon electrode," *International Journal of Electrochemical Science*, vol. 9, no. 12, pp. 7605–7613, 2014.
- [12] J. Sethi, M. Van Bulck, A. Suhail, M. Safarzadeh, A. Perez-Castillo, and G. Pan, "A label-free biosensor based on graphene and reduced graphene oxide dual-layer for electrochemical determination of beta-amyloid biomarkers," *Microchimica Acta*, vol. 187, no. 5, 2020, Art. no. 288.
- [13] S. Guo and E. Wang, "Synthesis and electrochemical applications of gold nanoparticles," *Analytica Chimica Acta*, vol. 598, no. 2, pp. 181–192, 2007.
- [14] J. M. Pingarrón, P. Yáñez-Sedeño, and A. González-Cortés, "Gold nanoparticle-based electrochemical biosensors," *Electrochimica Acta*, vol. 53, no. 19, pp. 5848–5866, 2008.
- [15] S. Shikha, K. G. Thakur, and M. S. Bhattacharyya, "Facile fabrication of lipase to amine functionalized gold nanoparticles to enhance stability and activity," *RSC Advances*, vol. 7, no. 68, pp. 42845–42855, 2017.
- [16] F. Zhang, S. Wang, and J. Liu, "Gold nanoparticles adsorb DNA and aptamer probes too strongly and a comparison with graphene oxide for biosensing," *Analytical Chemistry*, vol. 91, no. 22, pp. 14743–14750, 2019.
- [17] A. G. Semenov, A. B. Postnikov, N. N. Tamm, K. R. Seferian, N. S. Karpova, M. N. Bloshchitsyna, M. I. Krasnoselsky, D. V. Serebryanaya, and A. G. Katrukha, "Processing of pro-brain natriuretic peptide is suppressed by O-glycosylation in the region close to the cleavage site," *Clinical Chemistry*, vol. 55, no. 3, pp. 489–498, 2009.
- [18] C. D. Martin, G. Rojas, J. N. Mitchell, K. J. Vincent, J. Wu, J. McCafferty, and D. J. Schofield, "A simple vector system to improve performance and utilisation of recombinant antibodies," *BMC Biotechnol*, vol. 6, 2006, Art. no. 46.
- [19] O. Amor-Gutiérrez, E. Costa-Rama, N. Arce-Varas, C. Martínez-Rodríguez, A. Novelli, M.T. Fernández-Sánchez, and A. Costa-García, "Competitive electrochemical immunosensor for the detection of unfolded p53 protein in blood as biomarker for Alzheimer's disease," *Analytica Chimica Acta*, vol. 1093, pp. 28–34, 2020.
- [20] M. Jakubowska, "Signal processing in electrochemistry," *Electroanalysis*, vol. 23, no. 3, pp. 553–572, 2011.
- [21] J. L. Januzzi, Jr, C. A. Camargo, S. Anwaruddin, A. L. Baggish, A. A. Chen, D. G. Krauser, R. Tung, R. Cameron, J. T. Nagurney, C. U. Chae, D. M. Lloyd-Jones, D. F. Brown, S. Foran-Melanson, P. M. Sluss, E. Lee-Lewandrowski, and K. B. Lewandrowski, "The N-terminal Pro-BNP investigation of dyspnea in the emergency department (PRIDE) study," *American Journal of Cardiology*, vol. 95, no. 8, pp. 948–954, 2005.